Available online at www.sciencedirect.com
SCIENCE DIRECT
Virology 349 (2006) 364–275
VIROLOGY
www.elsevier.com/locate/yviro

Biochemical and functional characterization of the membrane association and membrane permeabilizing activity of the severe acute respiratory syndrome coronavirus envelope protein

Y. Liao [a], Q. Yuan [a], J. Torres [a], J.P. Tam [a], D.X. Liu [a,b,*]

[a] School of Biological Science, Nanyang Technological University, 60 Nanyang Drive, Singapore 637551, Singapore
[b] Institute of Molecular and Cell Biology, 61 Biopolis Drive, Proteos, Singapore 138673, Singapore

Received 1 November 2005; returned to author for revision 7 December 2005; accepted 21 January 2006
Available online 28 February 2006

Abstract

A diverse group of cytolytic animal viruses encodes small, hydrophobic proteins to modify host cell membrane permeability to ions and small molecules during their infection cycles. In this study, we show that expression of the SARS-CoV E protein in mammalian cells alters the membrane permeability of these cells. Immunofluorescent staining and cell fractionation studies demonstrate that this protein is an integral membrane protein. It is mainly localized to the ER and the Golgi apparatus. The protein can be translocated to the cell surface and is partially associated with lipid rafts. Further biochemical characterization of the protein reveals that it is posttranslationally modified by palmitoylation on all three cysteine residues. Systematic mutagenesis studies confirm that the membrane permeabilizing activity of the SARS-CoV E protein is associated with its transmembrane domain.

Keywords: SARS-CoV; E protein; Membrane association; Permeabilizing activity; Palmitoylation

Introduction

The causative agent of severe acute respiratory syndrome (SARS) was identified to be a novel coronavirus (SARS-CoV), an enveloped virus with a single strand, positive-sense RNA genome of 29.7 kb in length (Rota et al., 2003). In SARS-CoV-infected cells, a 3′-coterminal nested set of nine mRNA species, including the genome-length mRNA, mRNA 1, and eight subgenomic mRNAs (mRNA 2–mRNA 9), is produced (Thiel et al., 2003). Four structural proteins, spike (S), membrane (M), envelope (E), and nucleocapsid (N), arranged in the order 5′-S-E-M-N-3′, are encoded by subgenomic mRNA 2, 4, 5, and 9, respectively. In addition, 3a protein, a recently identified minor structural protein, is encoded by the first ORF of subgenomic mRNA3 (Ito et al., 2005; Yuan et al., 2005).

A group of small, highly hydrophobic viral proteins, termed viroporin, has been identified in diverse viral systems. These include the HCV p7 protein (Pavlovic et al., 2003), human immunodeficiency virus type 1(HIV-1) Vpu (Gonzalez and Carrasco, 1998; Schubert et al., 1996), influenza A virus M2 (Pinto et al., 1992), hepatitis A virus 2B (Jecht et al., 1998), semliki forest virus 6K (Sanz et al., 1994), picornavirus 2B (Agirre et al., 2002; Aldabe et al., 1996), chlorella virus PBCV-1 Kcv (Mehmel et al., 2003), and avian reovirus p10 protein (Bodelon et al., 2002). These proteins contain at least one transmembrane domain that interacts with and expands the lipid bilayer. The transmembrane domain could form hydrophilic pores in the membrane by oligomerization (Carrasco et al., 1995; Gonzalez and Carrasco, 2003). The hydrophilic channels would allow low molecular weight hydrophilic molecules to across the membrane barrier, leading to the disruption of membrane potential, collapse of ionic gradients, and release of essential compounds from the cell. Alterations in ion concentration would promote translation of viral versus cellular mRNAs, as translation of mRNAs from many cytolytic animal viruses is fairly resistant to high sodium concentrations

* Corresponding author. Institute of Molecular and Cell Biology, 61 Biopolis Drive, Proteos, Singapore 138673, Singapore.
E-mail address: dxliu@imcb.a-star.edu.sg (D.X. Liu).

0042-6822/$ - see front matter © 2006 Elsevier Inc. All rights reserved.
doi:10.1016/j.virol.2006.01.028

(Carrasco et al., 1995; Gonzalez and Carrasco, 2003). Progressive membrane damage during viral replication cycles would also result in cell lysis, promote viral budding and release, and facilitate virus spread to surrounding cells. Therefore, disruption of the function of viroporins could abrogate viral infectivity, rendering these proteins as suitable targets for the development of antiviral drugs.

Coronavirus E protein is a minor structural protein (Liu and Inglis, 1991; Yu et al., 1994). It plays essential roles in virion assembly, budding, morphogenesis, and regulation of other cellular functions (Corse and Machamer, 2001, 2002; Fischer et al., 1998; Lim and Liu, 2001). In a recent study, we demonstrated that the SARS-CoV E protein could obviously enhance the membrane permeability of bacterial cells to *o*-nitrophenyl-β-D-galactopyranoside and hygromycin B, suggesting that the protein may function as a viroporin (Liao et al., 2004). Similar observations were recently reported on mouse hepatitis virus E protein (Madan et al., 2005). In a separate study, the transmembrane domain of the protein was indeed shown to be able to form a cation channel on artificial membrane (Wilson et al., 2004). Molecular simulation and in vitro oligomerization studies indicate that this domain could form stable pentamers (Torres et al., 2005). In this study, we show that the expression of SARS-CoV E protein alters membrane permeability of mammalian cells. This membrane permeabilizing activity is associated with the transmembrane domain. Unlike in bacterial cells, mutations of the three cysteine residues alone do not obviously affect the membrane permeabilizing activity of the protein. Further biochemical characterization of the E protein shows that it is an integral membrane protein, and is posttranslationally modified by palmitoylation on all three cysteine residues.

Results

Alteration of membrane permeability to hygromycin B upon expression of SARS-CoV E protein in HeLa Cells

To test if the SARS-CoV E protein could affect the membrane permeability of mammalian cells, the Flag-tagged E protein was expressed in HeLa cells. At 12 h posttransfection, cells were treated with two different concentrations of hygromycin B for 30 min, and then radiolabeled with [^{35}S] methionine–cysteine for 3 h. Cell extracts were prepared and the expression of E protein was detected by immunoprecipitation with anti-Flag antibody under mild washing conditions. As shown in Fig. 1, extracts prepared from cells without treatment with hygromycin B showed the detection of the E protein and some other cellular proteins. In cells treated with 1 and 2 mM of hygromycin B, the expression of the E protein was reduced to 6 and 2%, respectively (Fig. 1). However, in cells transfected with the SARS-CoV N protein, a similar amount of the N protein was detected in cells both treated and untreated with hygromycin B (Fig. 1). The expression of the N protein was marginally reduced to 90 and 85%, respectively (Fig. 1). These results confirm that expression of E protein in mammalian cells alters the membrane permeability of these cells to hygromycin B.

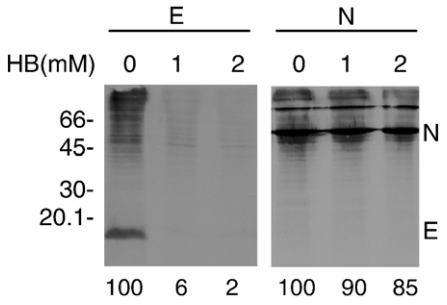

Fig. 1. Modification of the membrane permeability of mammalian cells by SARS-CoV E protein. HeLa cells expressing the Flag-tagged E protein were treated with 0, 1, and 2 mM of hygromycin B for 30 min at 12 h posttransfection (lanes 1, 2, and 3), and radiolabeled with [^{35}S] methionine–cysteine for 3 h. Cell lysates were prepared and the expression of E protein was detected by immunoprecipitation with anti-Flag antibody under mild washing conditions. Polypeptides were separated by SDS-PAGE and visualized by autoradiography. Cells expressing SARS-CoV N proteins were included as negative control (lanes 4, 5, and 6). The expression of N protein was detected by immunoprecipitation with polyclonal anti-N antibodies. The percentages of E and N proteins detected in the presence of hygromycin B were determined by densitometry and indicated at the bottom. Numbers on the left indicate molecular masses in kilodaltons.

Effects of mutations of the three cysteine residues on the membrane permeabilizing activity of the SARS-CoV E protein

SARS-CoV E protein contains three cysteine residues at amino acid positions 40, 43, and 44, respectively. These residues are located 3–7 amino acids downstream of the C-terminal residue of the transmembrane domain (Fig. 2). The first and third cysteine residues, at amino acid positions 40 and 44, respectively, were previously shown to play certain roles in oligomerization of the E protein (Liao et al., 2004). They may also be involved in the E protein-induced alteration of membrane permeability in bacterial cells (Liao et al., 2004). To systematically test the effects of these residues on the expression, posttranslational modification, folding, oligomerization, and the membrane-permeabilizing activities of E protein, seven mutants, C40-A, C43-A, C44-A, C40/44-A, C40/43-A, C43/44-A, and C40/43/44-A, with mutations of the three cysteine residues to alanine either individually or in combination of two or three, were made by site-directed mutagenesis (Fig. 2). Western blotting analysis of cells expressing wild type and most mutant constructs showed specific detection of three species migrating at the range of molecular masses from 14 to 18 kDa under reducing conditions and representing three isoforms of the E protein (Fig. 3a). These isoforms may be derived from posttranslational modification of the protein. The apparent molecular masses of these isoforms on SDS-PAGE are significantly larger than the calculated molecular mass of approximately 10 kDa for the Flag-tagged E protein.

In the membrane permeability assay shown in Fig. 3b, 0.5 and 1 mM of hygromycin B were used. The use of lower concentrations of hygromycin B is to ensure the detection of subtle changes on membrane permeability induced by the mutant constructs. Meanwhile, SARS-CoV N protein was cotransfected into HeLa cell together with wild type and mutant

```
                1         10        20        30        40        50        60        70
E               MYSFVSEETGTLIVNSVLLFLAFVVFLLVTLAILTALRLCAYCCNIVNVSLVKPTVYVYSRVKNLNSSEGVPDLLV
C40-A           ----------------------------------------A---------------------------------
C43-A           ----------------------------------------A---------------------------------
C44-A           ----------------------------------------A---------------------------------
C40/44-A        ----------------------------------------A---A-----------------------------
C40/43-A        ----------------------------------------A--A-----------------------------
C43/44-A        ----------------------------------------AA----------------------------------
C40/43/44-A     ----------------------------------------A--AA----------------------------------
Em1             ----------------EK-E--------------------------------------------------------
Em2             ------------------------E-KE------------------------------------------------
Em3             ----------------EK-----E-KE------------------------------------------------
Em4             ----------------EKEKEKE-----------------------------------------------------
Em5             --------------E-------------------------------------------------------------
Em6             ----------------EKEKEKE--------------A--AA----------------------------------
```

Fig. 2. Amino acid sequences of wild type and mutant SARS-CoV E protein. The putative transmembrane domain is underlined, and the three cysteine residues are in bold. Also indicated are the amino acid substitutions in each mutant construct.

E proteins to aid assessment of the inhibitory effect of protein synthesis by hygromycin B. Expression of wild type and mutant E protein showed that similar levels of inhibition of protein synthesis by hygromycin B were obtained (Fig. 3b). When 0.5 and 1 mM of hygromycin B were added to the culture medium, wild type and mutant E constructs render similar levels of inhibition to the expression of both N and E proteins (Fig. 3b). These results suggest that, contrary to the previous results observed in bacterial cells, these cysteine residues do not render significant effects on the membrane permeabilizing activity of the E protein. The reason for this discrepancy is uncertain, but it may reflect differences in posttranslational modifications, membrane association, subcellular localization, and translocation of the E protein in prokaryotic and eukaryotic cells.

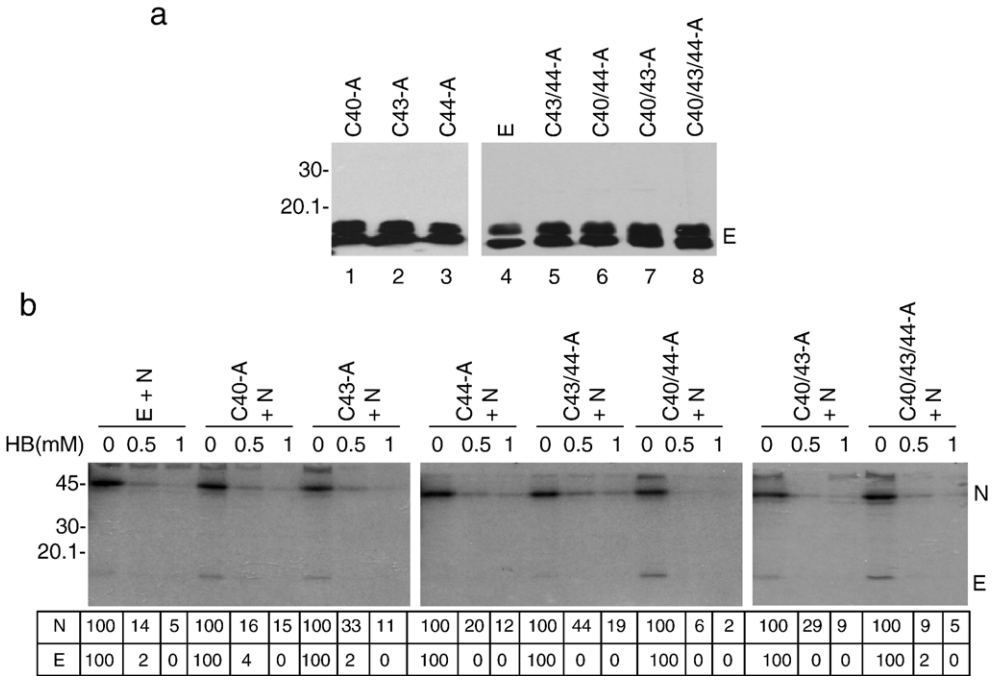

N	100	14	5	100	16	15	100	33	11	100	20	12	100	44	19	100	6	2	100	29	9	100	9	5
E	100	2	0	100	4	0	100	2	0	100	0	0	100	0	0	100	0	0	100	0	0	100	2	0

Fig. 3. Mutational analysis of the three cysteine residues of SARS-CoV E protein. (a) HeLa cells were transfected with the Flag-tagged wild type and seven mutant E constructs containing mutations of either a single (C40-A, C43-A, and C44-A), combination of two (C40/43-A, C40/44-A, and C43/44-A) or all three (C40/43/44-A) cysteine residues. Cell lysates were prepared at 24 h posttransfection, polypeptides were separated by SDS-PAGE and analyzed by Western blot using the anti-Flag antibody. Numbers on the left indicate molecular masses in kilodaltons. (b) Entry of hygromycin B into HeLa cells expressing wild type and mutant E proteins. HeLa cells expressing the Flag-tagged wild type E (lanes 1, 2, and 3) and seven cysteine to alanine mutation constructs (lanes 4–24) were treated with 0, 0.5, and 1 mM of hygromycin B for 30 min at 12 h posttransfection, and radiolabeled with [^{35}S] methionine–cysteine for 3 h. Cell lysates were prepared and the expression of E protein was detected by immunoprecipitation with anti-Flag antibody under mild washing conditions. SARS-CoV N protein was coexpressed with wild type and mutant E protein, and the expression of N protein was detected by immunoprecipitation with polyclonal anti-N antibodies. Polypeptides were separated by SDS-PAGE and visualized by autoradiography. The percentages of E and N proteins detected in the presence of hygromycin B were determined by densitometry and indicated at the bottom. Numbers on the left indicate molecular masses in kilodaltons.

Effects of mutations introduced into the transmembrane domain on the membrane permeabilizing activity of the SARS-CoV E protein

SARS-CoV E protein contains an unusually long putative transmembrane domain of 29 amino acid residues with a high leucine/isoleucine/valine content (55.17%) (Arbely et al., 2004). Recent molecular simulation and biochemical evidence showed that this domain may be involved in the formation of ion channel by oligomerization (Torres et al., 2005). Mutations of the putative transmembrane domain were therefore carried out to study its functions in membrane association and permeabilizing activity of the E protein. As shown in Fig. 2, four mutants, Em1, Em2, Em3, and Em4, were initially made by mutation of 3–7 leucine/valine residues to charged amino acid residues in the transmembrane domain. Two more mutants, Em5 and Em6, were subsequently made. Em5, which contains mutation of N15 to E, was constructed based on the molecular simulation studies showing that this residue may be essential for oligomerization of the protein (Fig. 2) (Torres et al., 2005). Em6 was made by combination of the Em4 and C40/43/44-A (Fig. 2). Expression of these mutants showed the detection of polypeptides with apparent molecular masses ranging from 10 to 18 kDa (Fig. 4a). Interestingly, mutations introduced into Em2, Em3, EM4, and Em6 significantly change the migration rate of the corresponding mutant E protein on SDS-PAGE. The apparent molecular mass of these mutants is approximately 10 kDa, which is consistent with the predicted molecular weight for the Flag-tagged E protein (Fig. 4a). The fact that substitutions of the hydrophobic amino acid residues in the transmembrane domain of the E protein with charged amino acids significantly alter the migrating properties of the E protein in SDS-PAGE may reflect the changes in overall conformation and membrane association of these mutants compared to wild type E protein.

In the hygromycin B permeability assays, cells transfected with Em1, Em2, and Em5 constructs showed a similar degree of inhibition on protein synthesis as in cells expressing wild type E protein (Fig 4b). In cells expressing Em3 and Em4, much less inhibition of protein synthesis by hygromycin B was observed compared to cells expressing wild type E protein (Fig. 4b). No obvious inhibition of protein synthesis was observed in cells expressing Em6 and N protein (Fig. 4b). These results confirm that the transmembrane domain is essential for the membrane permeabilizing activity of the protein, and further suggest that dramatic mutations of the transmembrane domain are required to disrupt this function. The combination of mutations in the transmembrane domain and the three cysteine residues abolishes the membrane permeabilizing activity of E protein, suggesting that these cysteine residues and may play certain roles in the membrane association and permeabilizing activity of the E protein.

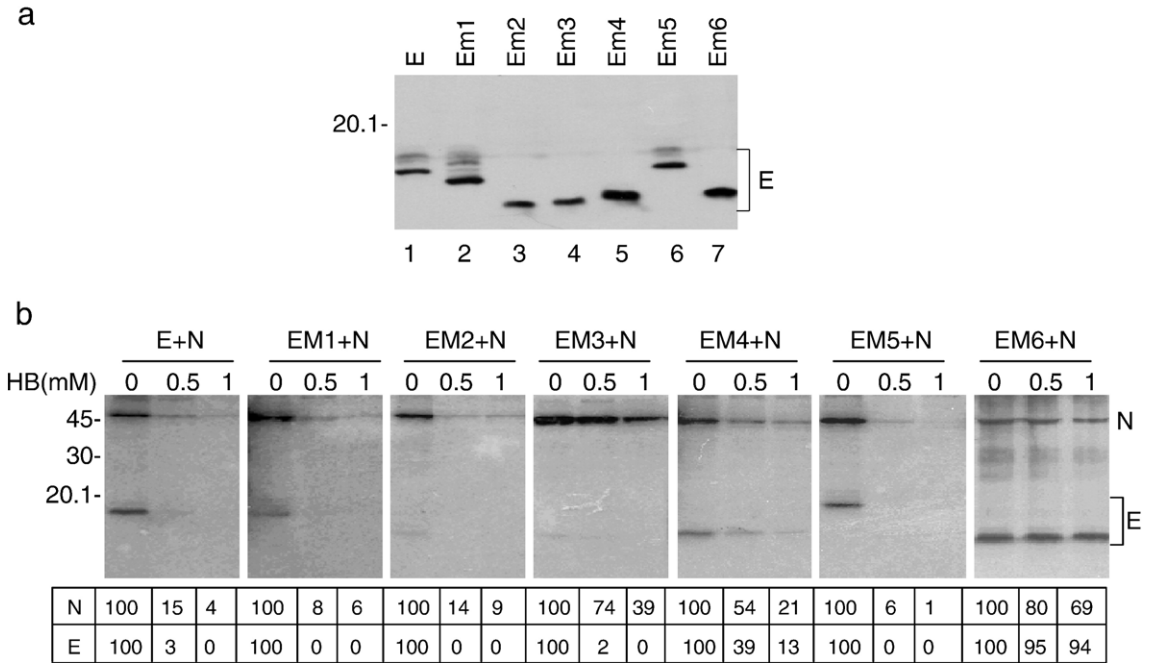

N	100	15	4	100	8	6	100	14	9	100	74	39	100	54	21	100	6	1	100	80	69
E	100	3	0	100	0	0	100	0	0	100	2	0	100	39	13	100	0	0	100	95	94

Fig. 4. Mutational analysis of the transmembrane domain of SARS-CoV E protein. (a) HeLa cells were transfected with the Flag-tagged wild type and six mutant constructs containing mutations in the transmembrane domain of the E protein. Cell lysates were prepared 24 h posttransfection, polypeptides were separated by SDS-PAGE and analyzed by Western blot using the anti-Flag antibody. Numbers on the left indicate molecular masses in kilodaltons. (b) Entry of hygromycin B into HeLa cells expressing wild type and mutant E proteins. HeLa cells expressing the Flag-tagged wild type E (lanes 1, 2, and 3) and six mutant E constructs (lanes 4–21), respectively, were treated with 0, 0.5, and 1 mM of hygromycin B for 30 min at 12 h posttransfection, and radiolabeled with [^{35}S] methionine–cysteine for 3 h. Cell lysates were prepared and the expression of E protein was detected by immunoprecipitation with anti-Flag antibody under mild washing conditions. SARS-CoV N protein was coexpressed with wild type and mutant E protein, and the expression of N protein was detected by immunoprecipitation with polyclonal anti-N antibodies. Polypeptides were separated by SDS-PAGE and visualized by autoradiography. The percentages of E and N proteins detected in the presence of hygromycin B were determined by densitometry and indicated at the bottom. Numbers on the left indicate molecular masses in kilodaltons.

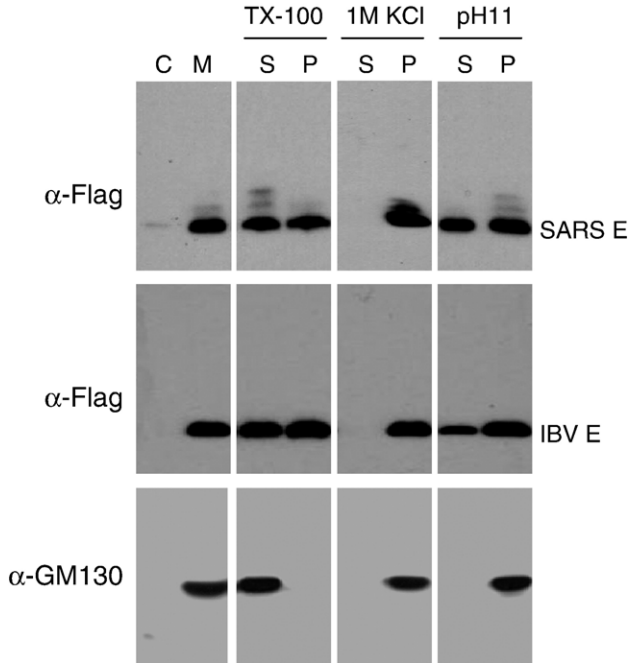

Fig. 5. Determination of SARS-CoV E protein as an integral membrane protein. HeLa cells expressing the Flag-tagged SARS-CoV and IBV E proteins, respectively, were harvested at 12 h posttransfection, broken by 20 stokes with a Dounce cell homogenizer, and fractionated into cytosol (C) and membrane (M) fractions after removal of cell debris and nuclei. The membrane fraction was treated with 1% Triton X-100, 100 mM Na_2CO_3 (pH 11), and 1 M KCl, respectively, and further fractionated into soluble (S) and pellet (P) fractions. Polypeptides were separated by SDS-PAGE and analyzed by Western blot using either anti-Flag antibody or anti-GM130 antibody (Abcam). Numbers on the left indicate molecular masses in kilodaltons.

Membrane association of SARS-CoV E protein

To characterize the membrane association property of the SARS-CoV E protein, HeLa cells expressing the Flag-tagged E protein were fractionated into membrane and cytosol fractions, and the presence of the E protein in each fraction was analyzed by Western blot. As shown in Fig. 5, the protein was almost exclusively located in the membrane fraction. Western blot analysis of the same fractions with anti-GM130 antibody (Abcam) showed the detection of an unknown host protein of approximately 60 kDa that is exclusively located in the membrane fraction (Fig. 5). Similarly, fractionation of HeLa cells expressing the Flag-tagged IBV E protein also showed exclusive detection of the protein in the membrane fraction (Fig. 5).

The membrane fraction was then treated with either 1% Triton X-100, 100 mM Na_2CO_3 pH 11 (high pH), or 1 M KCl (high salt), and centrifuged to separate the soluble contents (S) from the pellets (P). Treatment of the membrane fraction with 1 M KCl showed that both SARS-CoV and IBV E proteins were solely detected in the pellets (Fig. 5). Treatment of the same membrane pellets with 1% Triton X-100 and high pH led to the detection of the E proteins in both the supernatants and the pellets (Fig. 5). As an integral membrane protein control, anti-GM130 antibodies detected the protein exclusively in the supernatants after treatment of the membrane fraction with Triton X-100 (Fig. 5). In samples treated with both high pH and high salt, the protein was detected in the pellets only (Fig. 5), confirming that the procedures and conditions used to fractionate the cell lysates and to treat the membrane fractions are appropriate.

Oligomerization of SARS-CoV E protein

Oligomerization of viroporin is thought to be critical for the formation and expansion of the hydrophilic pore in the lipid bilayers. To determine the oligomerization status of the SARS-CoV E protein, the E protein with a His-tag at the C-terminus was expressed in insect cells using a baculovirus expression system and purified by Ni-NTA purification system. The purified E protein was concentrated and subjected to cross-linking with three different concentrations of glutaraldehyde, a short self-polymerizing reagent that reacts with lysine, tyrosine, histidine, and tryptophan. Cross-linking with glutaraldehyde showed the detection of dimer, trimer, tetramer, pentamer, and other higher-order oligomers/aggregates of the E protein under either non-reducing (Fig. 6, lanes 1–3) or reducing (Fig. 6, lanes 4–6) conditions. It was noted that more higher-order oligomers/aggregates were detected under non-reducing conditions when higher concentrations of the cross-linking reagent were used (Fig. 6, lanes 1–3). These results indicate that both interchain disulfide bond formation and hydrophobic interaction are contributing to the oligomerization of the E protein. More detailed characterization of the oligomerization status of the SARS-CoV E protein was hampered by the low expression efficiency of the protein in the system.

Palmitoylation of SARS-CoV E protein

The E protein from coronavirus MHV and IBV was previously shown to undergo modification by palmitoylation

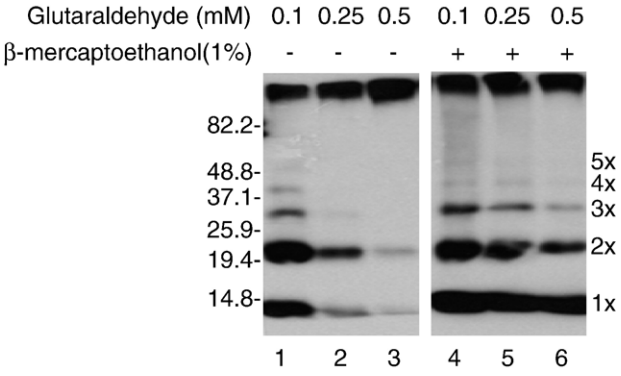

Fig. 6. Oligomerization of SARS-CoV E protein. The His-tagged E protein expressed in Sf9 insect cells was purified using Ni-NTA purification system (Qiagen), and incubated with three different concentrations of glutaraldehyde (0.1, 0.25, and 0.5 mM) for 1 h at room temperature. The reaction was quenched by adding 100 mM glycine. Polypeptides were separated on SDS-15% polyacrylamide gel in the presence or absence of 1% β-mercaptoethanol, and analyzed by Western blot with anti-His antibody. Different oligomers of the E protein are indicated on the right. Numbers on the left indicate molecular masses in kilodaltons.

(11, 43). To verify if SARS-CoV E protein is palmitoylated, two independent experiments were performed. First, treatment of the E protein with 1M hydroxylamine showed the reduced detection of the more slowly migrating isoforms (Fig. 7a, lanes 1 and 2). As a control, treatment of the IBV E protein with the same reagent abolished the detection of upper bands (Fig. 7a, lanes 3 and 4). Second, the three cysteine residues in combinations of two or all three were mutated to alanine (Fig. 2). Wild type and mutant E proteins were then expressed in HeLa cells and labeled with [^{3}H] palmitic acid or [^{35}S] methionine–cysteine. As shown in Fig. 7b, wild type and all mutant E proteins were efficiently labeled with [^{35}S] methionine–cysteine (Fig. 7b, upper panel). In cells labeled with [^{3}H] palmitate, wild type and the three mutants with mutations of different combinations of two cysteine residues (C40/44-A, C40/43-A and C43/44-A) were efficiently detected (Fig. 7b, lower panel, lanes 1–4). However, the construct with mutation of all three cysteine residues (C40/43/44-A) was not labeled (Fig. 7b, lower panel, lane 5). As a positive control, the IBV E protein was also efficiently labeled by [^{3}H] palmitate (Fig. 7b, lower panel, lane 6). These results confirm that SARS-CoV E protein is modified by palmitoylation at all three cysteine residues.

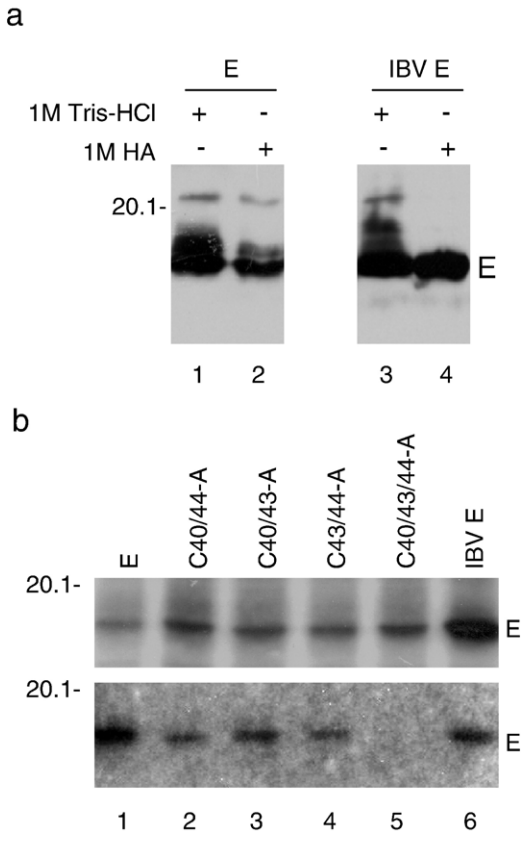

Fig. 7. Palmitoylation of SARS-CoV E protein. (a) Total cell lysates prepared from HeLa cells expressing the Flag-tagged SARS-CoV E protein (lanes 1 and 2) and IBV E protein (lanes 3 and 4) were treated either with 1 M Tris–HCl (lanes 1 and 3) or 1M hydroxylamine (lanes 2 and 4). Polypeptides were separated by SDS-PAGE and analyzed by Western blot using the anti-Flag antibody. Numbers on the left indicate molecular masses in kilodaltons. (b) HeLa cells expressing the Flag-tagged wild type SARS-CoV E protein (lane 1), mutant C40/44-A (lane 2), C40/44-A (lane 3), C43/44-A (lane4), C40/43/44-A (lane 5), and IBV E protein (lane 6) were radiolabeled with [^{35}S] methionine–cysteine (upper panel) and [^{3}H] palmitic acid (lower panel). Cell lysates were prepared and subjected to immunoprecipitation with anti-Flag antibody. Polypeptides were separated by SDS-PAGE and visualized by autoradiography. Numbers on the left indicate molecular masses in kilodaltons.

Mutational analysis of the subcellular localization and membrane association property of SARS-CoV E protein

To further analyze the membrane association properties of the E protein, its subcellular localization was studied by indirect immunofluorescence. HeLa cells overexpressing the Flag-tagged E protein were fixed with 4% paraformaldehyde at 12 h postinfection and stained with anti-Flag monoclonal antibody (Fig. 8a). In cells permeabilized with 0.2% Triton X-100, the Flag-tagged E protein is mainly localized to the perinuclear regions of the cells (Fig. 8a, panel A). The staining patterns largely overlap with calnexin, an ER resident protein (panels B and C). It was also noted that some granules and punctated staining patterns are not well merged with the calnexin staining patterns. They may represent aggregates of the E protein.

The exact subcellular localization of a coronavirus E protein is an issue of debate in the current literature (Corse and Machamer, 2003). Although clear ER localization of the coronavirus IBV E protein was observed at early time points in a time course experiment using an overexpression system (Lim and Liu, 2001), no such localization patterns were observed as reported by Corse and Machamer (2003). To clarify that the above observed ER localization pattern may be due to the high expression level of the protein in HeLa cells using the vaccinia/T7 system, the subcellular localization of the SARS-CoV E protein in another cell type with lower expression efficiency of the protein was carried out. As shown in Fig. 8a, expression of the Flag-tagged SARS-CoV in BHK cells stably expressing the T7 RNA polymerase (Buchholz et al., 1999) showed that the protein exhibits typical Golgi localization patterns (panels D–F). Expression of the untagged SARS-CoV E protein in the same cell type also shows very similar Golgi localization patterns as the Flag-tagged protein (Fig. 8a, panels G–I). These results suggest that the predominant ER localization patterns in HeLa cells observed above may be due to the cell type used and the very high expression levels of the protein in individual cells with the vaccinia/T7 expression system.

The subcellular localization of wild type and six mutants, Em1, Em2, Em3, Em4, Em5, and Em6, was then studied in BHK cells. The localization patterns of Em1, Em2, and Em5 were similar to wild type E protein, showing predominant Golgi localization patterns (Fig. 8b). In cells expressing Em3 and Em4, more diffuse staining patterns throughout the cytoplasm were observed (Fig. 8b). It suggests that these mutations may change the membrane association properties of the protein, leading to the alteration of the subcellular localization of the

protein. In cells expressing Em6, a diffuse localization pattern was observed (Fig. 8b).

The membrane association properties of wild type and mutant E proteins were further confirmed by fractionation of HeLa cells expressing E protein into membrane and cytosol fractions, and the presence of E protein in each fraction was analyzed by Western blot. As shown in Fig. 8c, 95.28% of wild type E protein was detected in the membrane fraction. The percentages of the mutant E protein detected in the similarly prepared membrane fraction were 93.67% for Em1, 89.85% for Em2, 62.60% for Em3, 58.58%for Em4, 93.64% for Em5, and 55.46% for Em6 (Fig. 8c).

Partial association of SARS-CoV E protein with lipid rafts

To test if the E protein may be associated with lipid rafts, the low-density, detergent-insoluble membrane fraction was isolated from HeLa cells overexpressing the SARS-CoV E protein. As shown in Fig. 9, the majority of the E protein was detected at the bottom fractions (lanes 9–11). However, a certain proportion of E protein associated with lipid rafts was detected in fractions 3, 4, and 5 (Fig. 9, lanes 3–5). As a marker for lipid rafts, the GM1 was detected in fractions 4 and 5 (Fig. 9, lanes 3 and 4).

Discussion

All coronaviruses encode a small hydrophobic envelope protein with essential functions in virion assembly, budding, and morphogenesis (Corse and Machamer, 2001, 2002; Fischer et al., 1998; Lim and Liu, 2001). In a previous study, the SARS-CoV E protein was shown to obviously enhance the membrane permeability of bacterial cells to *o*-nitrophenyl-β-D-galactopyranoside and hygromycin B (Liao et al., 2004). In this study, we show that this protein can also alter membrane permeability of mammalian cells to the general translation inhibitor, hygromycin B. Evidence present further demonstrates that the SARS-CoV E protein is an integral membrane protein, and its membrane-permeabilizing activity is associated with the transmembrane domain. The

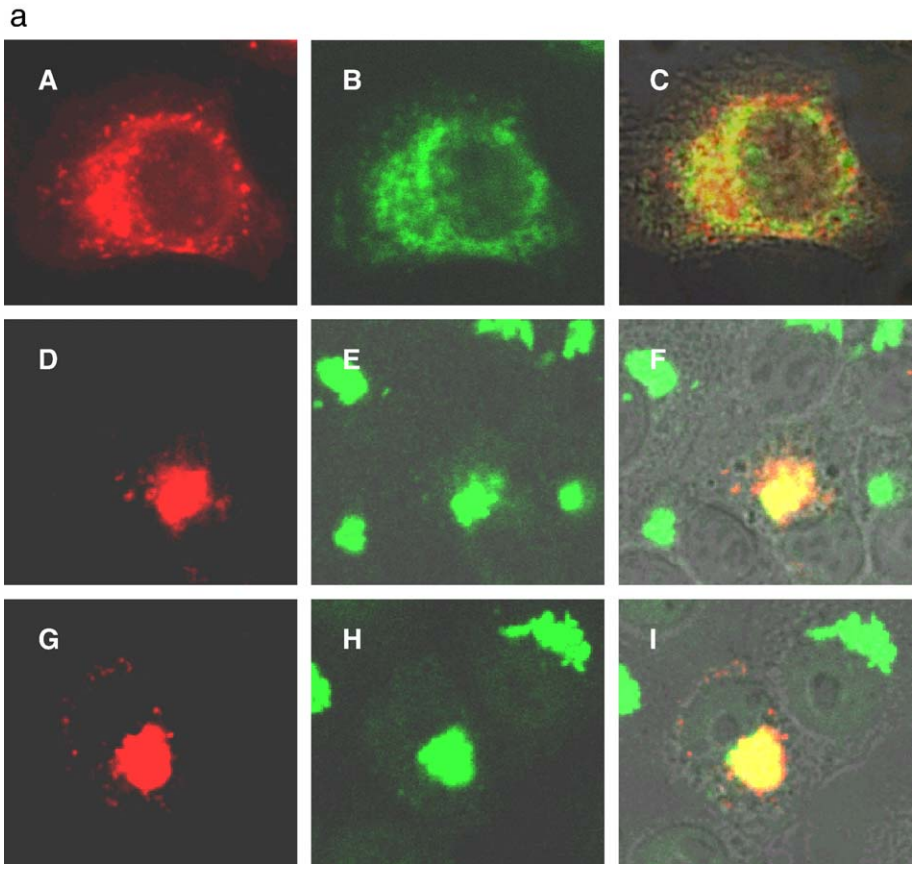

Fig. 8. Subcellular localization and membrane association of wild type and mutant SARS-CoV E protein. (a) HeLa cells expressing the Flag-tagged E protein (A–C), and BHK cells expressing the Flag-tagged (D–F) and untagged (G–I) SARS-CoV E were stained with either anti-Flag (A–F) or anti-E (G–I) antibodies at 12 h posttransfection after permeabilizing with 0.2% Triton X-100. The same HeLa cells were also stained with anti-calnexin antibody (B), and the same BHK cells were also stained with anti-p230 trans Golgi antibodies (panels E and H). Panels C, F, and I show the overlapping images. (b) BHK cells expressing the Flag-tagged wild type (E) and mutant E protein (Em1, Em2, Em3, Em4, Em5, and Em6) were stained with anti-Flag antibody at 12 h posttransfection after permeabilizing with 0.2% Triton X-100. (c) HeLa cells expressing the Flag-tagged wild type and mutant E protein were harvested at 12 h posttransfection, broken by 20 stokes with a Dounce cell homogenizer, and fractionated into cytosol (C) and membrane (M) fractions after removal of cell debris and nuclei. Polypeptides were separated by SDS-PAGE and analyzed by Western blot using the anti-Flag antibody. The percentages of E protein detected in the membrane fraction were determined by densitometry and indicated on the right. Numbers on the left indicate molecular masses in kilodaltons.

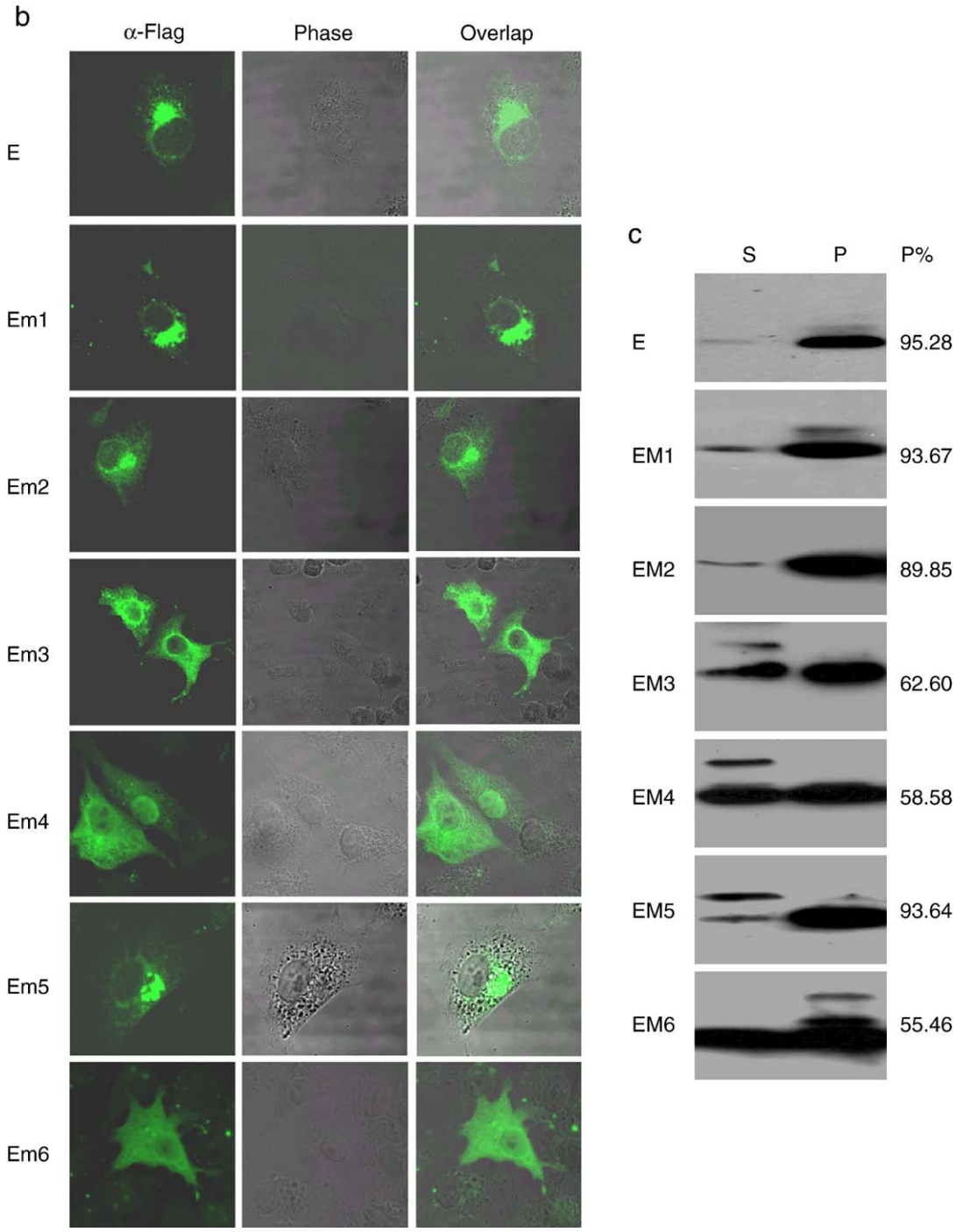

Fig. 8 (*continued*).

protein is posttranslationally modified by palmitoylation on all the three cysteine residues.

SARS-CoV E protein contains a putative long transmembrane domain of 29 amino acid residues (Arbely et al., 2004). In a recent report, Arbely et al. (2004) showed that the protein might have a highly unusual topology, consisting of a short transmembrane helical hairpin that forms an inversion about a previously unidentified pseudo-center of symmetry. This hairpin structure could deform lipid bilayers and cause tabulation (Arbely et al., 2004). The full-length and N-terminal 40 amino acid region were shown to be able to form cation-selective ion channels on artificial lipid bilayers (Wilson et al., 2004). By using molecular simulation and synthetic peptide approaches, it was shown that the transmembrane domain of E protein could form ion channels by homooligomerization into stable dimers, trimers, and pentamers (Torres et al., 2005). The mutagenesis data present in this study showed that introduction of radical mutations to the transmembrane domain is required to block the membrane-permeabilizing activity of the protein.

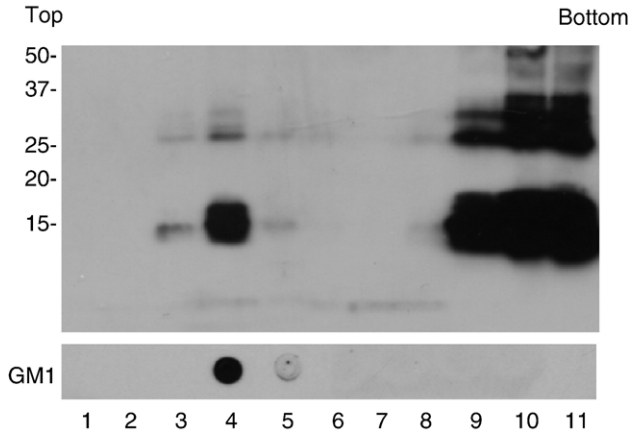

Fig. 9. Association of SARS-CoV E protein with lipid rafts. HeLa cells expressing the Flag-tagged SARS E protein were lysed with 1% Triton, and centrifuged to remove insoluble material and nuclei. The supernatants were fractionated by ultracentrifugation with a sucrose gradient, and 11 fractions were collected. The presence of the SARS-CoV E protein in each fraction was analyzed by Western blot using anti-Flag antibody, and the presence of GM1 was determined by dot blot. Numbers on the left indicate molecular masses in kilodaltons.

Mutations introduced into the transmembrane domain of SARS-CoV E protein in Em2 as well as in Em3 and Em4 drastically change the migration properties of the E protein in SDS-PAGE (Fig. 4a). It suggests that these mutations would have significantly altered the overall folding, hydrophobicity, and membrane association properties of the E protein. However, this mutant shows very similar properties in subcellular localization, membrane association, and membrane-permeabilizing activity as wild type E protein. The high tolerance of E protein to such dramatic mutations indicates that maintenance of these properties would be essential for the functionality of E protein in coronavirus life cycles. This possibility would warrant more systematic studies by using an infectious clone system.

The first and third Cys residues of the E protein were previously shown to play important roles in oligomerization and modification of membrane permeability in bacterial cells (Liao et al., 2004). The protein could form homodimers and trimers by interchain disulfide bonds in both bacterial and mammalian cells (Liao et al., 2004). In this study, mutation of all the three cysteine residues did not obviously affect the membrane-permeabilizing activity of the E protein. Instead, these residues could affect the membrane association of the protein as they were shown to be modified by palmitoylation. Examples of palmitoylation of viral and cellular proteins on multiple cysteine residues include influenza virus HA protein, members of seven transmembrane domains containing G-protein-coupled receptors (CCR5 and endothelin B receptor, etc.), and other cellular proteins (Bijlmakers and Marsh, 2003).

Lipid modification by palmitic acid has been reported for a number of viral envelope proteins, including the hemagglutinin (HA) and M2 protein of influenza virus (Melkonian et al., 1999; Schroeder et al., 2004; Veit et al., 1991; Zhang et al., 2000), gp160 of HIV-1 (Rousso et al., 2000), and Env protein of murine leukemia virus (Li et al., 2002). The E protein of coronavirus mouse hepatitis virus and IBV was also reported to be palmitoylated (Corse and Machamer, 2001). It has been noted that palmitoylation of viral envelope proteins usually takes place on cysteine residues located within the transmembrane domain or in the cytoplasmic tail close to this domain (Bhattacharya et al., 2004; Hausmann et al., 1998; Schmidt et al., 1988; Veit et al., 1989). This thioester linkage of fatty acids to viral envelope proteins is a posttranslational event that takes place in the *cis* or medial Golgi after exit from the ER and after oligomerization but prior to acquisition of endo H (endo-β-*N*-acetylglucosaminidase H) resistance (Bonatti et al., 1989; Veit and Schmidt, 1993). Palmitoylation of viral proteins plays a considerable role in virus infectivity, virion assembly, and release. For example, palmitoylation of the HA protein of influenza virus enhances its association with lipid rafts (Melkonian et al., 1999; Zhang et al., 2000); palmitoylation of the HIV-1 envelope glycoprotein is critical for viral infectivity (Rousso et al., 2000); palmitoylation of the murine leukemia virus envelope protein is critical for its association with lipid rafts and cell surface expression (Li et al., 2002); palmitoylation of the Rous sarcoma virus transmembrane glycoprotein is required for protein stability and virus infectivity (Ochsenbauer-Jambor et al., 2001). The observed palmitoylation of the SARS-CoV E protein may play certain roles in its cell surface expression and association with lipid rafts.

In this study, we show that radical mutations introduced into the transmembrane domain of the SARS-CoV E protein could neither totally block the membrane-permeabilizing activity nor completely disrupt the membrane association properties of the protein, unless the three cysteine residues were simultaneously mutated. This may reflect the relatively low sensitivity of the hygromycin B assays used to detect the membrane-permeabilizing activity of the protein. Alternatively, it suggests that the palmitoylated mutant E protein may be still tightly associated with cellular membrane, as palmitoylation of the protein would help target the protein to the cellular membrane. This membrane association could, in turn, cause membrane damage, leading to the increased membrane permeability to hygromycin B.

Subcellular fractionation and biochemical characterization studies demonstrated that, similar to the IBV E protein, the SARS-CoV E protein behaves as an integral membrane protein. However, it was consistently observed that, under the experimental conditions used, certain proportions of both SARS-CoV and IBV E proteins associated with cellular membranes were resistant to 1% Triton X-100, while some of the membrane-associated proteins can be released from the membrane pellets by treatment with high pH. Two possibilities are considered. First, as observed in this study, SARS-CoV E protein is partially associated with lipid rafts. This may render the protein resistant to the treatment by Triton X-100. Second, immunofluorescent staining of cells expressing the E protein showed the detection of the protein with punctated staining patterns at both cell surface and intracellular structures. It would suggest that the protein may form aggregates. These aggregates

may be cofractionated with the membrane-associated E protein and can be released by high pH but are resistant to the detergent treatment.

Cell surface expression is a prerequisite for SARS-CoV E protein to alter the membrane permeability of the cells. Over the course of this study, it was consistently observed that SARS-CoV E protein exhibits much weaker cell surface staining than the IBV E protein even in cells overexpressing the protein (data not shown). This may reflect the unique topology of the SARS-CoV E protein on cellular membranes. This possibility is currently under investigation.

Material and methods

Polymerase chain reaction and site-directed mutagenesis

Amplification of respective template DNAs with appropriate primers was performed with Pfu DNA polymerase (Strategene) with 2 mM $MgCl_2$. The PCR conditions were 35 cycles of 94 °C for 45 s, 46–58 °C for 45 s, and 72 °C for 30 s. The annealing temperature and extension time were subjected to adjustments according to the melting temperatures of the primers used and the lengths of the PCR fragments synthesized.

Site-directed mutagenesis was carried out with two rounds of PCR and two pairs of primers (Liu et al., 1997).

Transient expression of SARS-CoV sequence in mammalian cells

HeLa cells were grown at 37 °C in 5% CO_2 and maintained in Glasgow's modified Eagle's medium supplemented with 10% fetal calf serum. SARS-CoV E and mutants were placed under the control of a T7 promoter and transiently expressed in mammalian cells using a vaccinia virus-T7 expression system. Briefly, 60–80% confluent monolayers of HeLa cells grown on dishes (Falcon) were infected with 10 plaque-forming units/cell of a recombinant vaccinia virus (vTF7-3) that expresses T7 RNA polymerase. Two hours later, cells were transfected with plasmid DNA mixed with Effectene according to the instructions of the manufacturer (Qiagen). Cells were harvested at 12 to 24 h posttransfection.

Western blot analysis

Total proteins extracted from HeLa cells were lysed with 2× SDS loading buffer in the presence of 200 mM DTT plus 10 mM of iodoacetamide and subjected to SDS-PAGE. Proteins were transferred to PVDF membrane (Stratagene) and blocked overnight at 4 °C in blocking buffer (5% fat free milk powder in PBST buffer). The membrane was incubated with 1:2000 diluted primary antibodies in blocking buffer for 2 h at room temperature. After washing three times with PBST, the membrane was incubated with 1:2000 diluted anti-mouse or anti-rabbit IgG antibodies conjugated with horseradish peroxidase (DAKO) in blocking buffer for 1 h at room temperature. After washing for three times with PBST, the polypeptides were detected with a chemiluminescence detection kit (ECL, Amersham Biosciences) according to the instructions of the manufacturer.

Metabolic radiolabeling, immunoprecipitation, and SDS-PAGE

Permeability of the plasma membrane of cells expressing SARS-CoV E or mutants to hygromycin B was determined as described below. Briefly, HeLa cells in 100 mm dish were transfected with plasmids described as above, the cells were pretreated with different concentrations of hygromycin B (Sigma) for 30 min in methionine–cysteine free medium at 12 h posttransfection, and then 25 μCi/ml of [^{35}S] methionine–cysteine (Amersham) was added to the culture medium. The cells were incubated at 37 °C for 3 h in the presence or absence of hygromycin B, harvested, and lysed in 1× radioimmune precipitation assay buffer (RIPA) containing 1.0 mM phenylmethylsulfonyl fluoride and 10 μg/ml each of aprotinin and leupeptin (Roche Applied Science). The cell extracts were clarified for 10 min at 13,000 rpm at 4 °C, and the proteins were immunoprecipitated with appropriate antibodies for 1 h at 4 °C, incubated with 20 μl of protein A-agarose overnight at 4 °C, and washed three times with RIPA. The proteins were analyzed by 15% SDS-PAGE.

For palmitoylation assay, HeLa cells in 60mm dish were labeled with 1 mCi/ml of [9, 10-^{3}H] palmitic acid (50Ci/mmol; Amersham) for 10 h at 4 h posttransfection. A duplicate dish of cells was labeled with 25 μCi/ml of [^{35}S] methionine–cysteine (Amersham) for 10 h at 4 h posttransfection. Cells were harvested and proteins were immunoprecipitated as described above.

Expression and purification of the SARS-CoV E protein expressed in insect cells

A cDNA fragment covering the SARS-CoV E protein with a His-tag at the C-terminus was cloned to the transfer vector pVL1392 (Pharmingen). A recombinant baculovirus expressing the His-tagged SARS-CoV E protein was generated by cotransfection of the pVL1392-E-His construct together with Baculogold DNA (Pharmingen) into Sf9 cells according to the instruction of the manufacturer. Fresh Sf9 cells were infected with the recombinant virus and harvested at 72 h postinfection. The His-tagged E protein was purified using Ni-NTA purification system (Qiagen) according to the instruction of the manufacturer.

Cross-linking experiment

The His-tagged E protein was incubated with 0.1, 0.25, and 0.5 mM glutaraldehyde at room temperature for 1 h. The reaction was quenched by adding 100 mM glycine. Polypeptides were separated on SDS-15% polyacrylamide gel in the presence or absence of 1% β-mercaptoethanol, and analyzed by Western blot with anti-His antibody.

Indirect immunofluorescence

HeLa cells expressing E protein or various mutants were fixed with 4.0% paraformaldehyde for 10 min at 16 h post-transfection, washed three times with 1× PBS, permeabilized with 0.2% Triton X-100 for 10 min at room temperature, and washed three times with 1× PBS. Rabbit anti-E antibodies were used to detect E protein and mutants, and mouse anti-calnexin monoclonal antibodies (Abcam) were used to detect calnexin, an ER marker. Mouse anti-Flag monoclonal antibodies were also used to detect Flag-tagged E protein and mutants.

Subcellular fractionation

HeLa cells were resuspended in hypotonic buffer (1 mM Tris–HCl pH 7.4, 0.1 mM EDTA, 15 mM NaCl) containing 2 μg of leupeptin per ml and 0.4 mM phenylmethylsulfonyl fluoride and broken by 20 strokes with a Dounce cell homogenizer. Cell debris and nuclei were removed by centrifugation at 1500 × *g* for 10 min at 4 °C. The cytosol fraction and membrane fraction (postnuclear fraction) were separated by ultracentrifugation through a 6% sucrose cushion at 150,000×*g* for 30 min at 4 °C. Membrane pellets were resuspended in hypotonic buffer, treated with 1% Triton X-100, 100 mM Na_2CO_3 or 1 M KCl for 30 min, and further fractionated into supernatant (S) and pellet (P) fractions by ultracentrifugation at 150,000 × *g* for 30 min at 4 °C.

Isolation of low-density detergent-insoluble membrane fractions on flotation gradients

HeLa cells expressing the Flag-tagged SARS-C0V E from two 10 cm dishes were washed twice with ice-cold PBS and lysed on ice for 30 min in 1 ml of 1% Triton X-100 TNE lysis buffer (25 mM Tris–HCl pH 7.5, 150 mM NaCl, 5 mM EDTA) supplemented with protease inhibitor cocktail (Roche). The cell lysates were homogenized with 25 strokes using a Dounce homogenizer and centrifuged at 3000 × *g* at 4 °C for 5 min to remove insoluble materials and nuclei. The supernatants were mixed with 1 ml of 80% sucrose in lysis buffer, placed at the bottom of a ultracentrifuge tube, overlaid with 6 ml of 30% and 3 ml of 5% sucrose in TNE lysis buffer, and ultracentrifuged at 38,000 rpm at 4 °C in a SW41 rotor (Beckman) for 18 h. After centrifugation, 11 fractions (1 ml each) were collected from the top to the bottom and analyzed immediately by Western blot or stored at −80 °C.

Construction of plasmids

Plasmid pFlagE was constructed by cloning an *Eco*RV- and *Eco*RI-digested PCR fragment into *Eco*RV- and *Eco*RI-digested pFlag. The Flag tag is fused to the N-terminal end of the E protein. The two primers used are: 5′-CGGGATATCCTACTCATTCGTTT CGGAA-3′ and 5′-CCGGAATTCTTAGACCAGAAGATCAGGAAC-3′. Mutations were introduced into the E gene by two rounds of PCR. The PCR amplified fragments were cloned into *Eco*RV- and *Eco*RI-digested pFlag. All plasmids and the introduced mutations were confirmed by automated DNA sequencing.

Acknowledgments

This work was supported by the Agency for Science Technology and Research, Singapore and a grant the Biomedical Research Council (BMRC 03/1/22/17/220).

References

Agirre, A., Barco, A., Carrasco, L., Nieva, J.B., 2002. Viroporin-mediated membrane permeabilization. J. Biol. Chem. 277, 40434–40441.

Aldabe, R., Barco, A., Corrasco, L., 1996. Membrane permeabilization by poliovirus proteins 2B and 2BC. J. Biol. Chem. 271, 23134–23137.

Arbely, E., Khattari, Z., Brotons, G., Akkawi, M., Salditt, T., Arkin, I.T., 2004. A highly unusual palindromic transmembrane helical hairpin formed by SARS coronavirus E protein. J. Mol. Biol. 341, 769–779.

Bhattacharya, J., Peters, P.J., Clapham, P.R., 2004. Human immunodeficiency virus type 1 envelope glycoproteins that lack cytoplasmic domain cysteines: impact on association with membrane lipid rafts and incorporation onto budding virus particles. J. Virol. 78, 5500–5506.

Bijlmakers, M.-J., Marsh, M., 2003. The on–off story of protein palmitoylation. Trends Cell Biol. 13, 32–42.

Bodelon, G., Labrada, L., Martinez-Costas, J., Benavente, J., 2002. Modification of late membrane permeability in avian reovirus-infected cells. J. Biol. Chem. 227, 17789–17796.

Bonatti, S., Migliaccio, G., Simons, K., 1989. Palmitoylation of viral membrane glycoproteins takes place after exit from the endoplasmic reticulum. J. Biol. Chem. 264, 12590–12595.

Buchholz, U.J., Finke, S., Conzelmann, K.K., 1999. Generation of bovine respiratory syncytial virus (BRSV) from cDNA: BRSV NS2 is not essential for virus replication in tissue culture, and the human RSV leader region acts as a functional BRSV genome promoter. J. Virol. 73, 251–259.

Carrasco, L., Perez, L., Irurzun, A., Lama, J., Martinez-Abarca, F., Rodriguez, P., Guinea, R., Castrillo, J.L., Sanz, M.A., Ayala, M.J., 1995. Modification of membrane permeability by animal viruses. Adv. Virus Res. 45, 61–112.

Corse, E., Machamer, C.E., 2001. Infectious bronchitis virus E protein is targeted to the Golgi complex and directs release of virus-like particles. J. Virol. 74, 4319–4326.

Corse, E., Machamer, C.E., 2002. The cytoplasmic tail of infectious bronchitis virus E protein directs Golgi targeting. J. Virol. 76, 1273–1284.

Corse, E., Machamer, C.E., 2003. The cytoplasmic tails of infectious bronchitis virus E and M proteins mediate their interaction. Virology 312, 25–34.

Fischer, F., Stegen, C.F., Masters, P.S., Samsonoff, W.A., 1998. Analysis of constructed E gene mutants of mouse hepatitis virus confirms a pivotal role for E protein in coronavirus assembly. J. Virol. 72, 7885–7894.

Gonzalez, M.E., Carrasco, L., 1998. The human immunodeficiency virus type 1 vpu protein enhances membrane permeability. Biochemistry 37, 13710–13719.

Gonzalez, M.E., Carrasco, L., 2003. Viroporins. FEBS Lett. 552, 28–34.

Hausmann, J., Ortmann, D., Witt, E., Veit, M., Seidel, W., 1998. Adenovirus death protein, a transmembrane protein encoded in the E3 region, is palmitoylated at the cytoplasmic tail. Virology 244, 343–351.

Ito, N., Mossel, E.C., Narayanan, K., Popov, V.L., Huang, C., Inoue, T., Peters, C.J., Makino, S., 2005. Severe acute respiratory syndrome coronavirus 3a protein is a viral structural protein. J. Virol. 79, 3182–3186.

Jecht, M., Probst, C., Gauss-Muller, V., 1998. Membrane permeability induced by Hepatitis A virus proteins 2B and 2BC and proteolytic processing of HAV 2BC. Virology 252, 218–227.

Li, M., Yang, C., Tong, S., Weidmann, A., Compans, R.W., 2002. Palmitoylation of the murine leukemia virus envelope protein is critical for lipid raft association and surface expression. J. Virol. 76, 11845–11852.

Liao, Y., Lescar, J., Tam, J.P., Liu, D.X., 2004. Expression of SARS-coronavirus envelope protein in *Escherichia coli* cells alters membrane permeability. Biochem. Biophys. Res. Commun. 325, 374–380.

Lim, K.P., Liu, D.X., 2001. The missing link in coronavirus assembly. J. Biol. Chem. 276, 17515–17523.

Liu, D.X., Inglis, S.C., 1991. Association of the infectious bronchitis virus3c protein with the virion envelope. Virology 185, 911–917.

Liu, D.X., Xu, H.Y., Brown, T.D.K., 1997. Proteolytic processing of the coronavirus infectious bronchitis virus 1a Polyprotein: identification of a 10-kilodalton polypeptide and determination of its cleavage sites. J. Virol. 71, 1814–1820.

Madan, V., Garcia, M.J., Sanz, M.A., Carrasco, L., 2005. Viroporin activity of murine hepatitis virus E protein. FEBS Lett. 579, 3607–3612.

Mehmel, M., Rothermel, M., Meckel, T., Van Etten, J.L., Moroni, A., Thiel, G., 2003. Possible function for virus encoded K+ channel Kcv in the replication of chlorella virus PBCV-1. FEBS Lett. 552, 7–11.

Melkonian, K.A., Ostermeyer, A.G., Chen, J.Z., Roth, M.G., Brown, D.A., 1999. Role of lipid modifications in targeting proteins to detergent-resistant membrane rafts. Many raft proteins are acylated, while few are prenylated. J. Biol. Chem. 274, 3910–3917.

Ochsenbauer-Jambor, C., Miller, D.C., Roberts, C.R., Rhee, S.S., Hunter, E., 2001. Palmitoylation of the Rous sarcoma virus transmembrane glycoprotein is required for protein stability and virus infectivity. J. Virol. 75, 11544–11554.

Pavlovic, D., Neville, D.C.A., Argaud, O., Blumberg, B., Dwek, R.A., Fischer, W.B., Zitzmann, N., 2003. The hepatitis C virus forms an ion channel that is inhibited by long-alkyl-chain iminosugar derivatives. Proc. Natl. Acad. Sci. 100, 6104–6108.

Pinto, L.H., Holsinger, L.J., Lamb, R.A., 1992. Influenza virus M2 protein has ion channel activity. Cell 59, 517–528.

Rota, P.A., Oberste, M.S., Monroe, S.S., Nix, W.A., Campagnoli, R., Icenogle, J.P., Penaranda, S., Bankamp, B., Maher, K., Chen, M.H., Tong, S., Tamin, A., Lowe, L., Frace, M., DeRisi, J.L., Chen, Q., Wang, D., Erdman, D.D., Peret, T.C., Burns, C., Ksiazek, T.G., Rollin, P.E., Sanchez, A., Liffick, S., Holloway, B., Limor, J., McCaustland, K., Olsen-Rasmussen, M., Fouchier, R., Gunther, S., Osterhaus, A.D., Drosten, C., Pallansch, M.A., Anderson, L.J., Bellini, W.J., 2003. Characterization of a novel coronavirus associated with severe acute respiratory syndrome. Science 300, 1394–1399.

Rousso, I., Mixon, M.B., Chen, B.K., Kim, P.S., 2000. Palmitoylation of the HIV-1 envelope glycoprotein is critical for viral infectivity. Proc. Natl. Acad. Sci. 97, 13523–13525.

Sanz, M.A., Perez, L., Carrasco, L., 1994. Semliki forest virus 6K protein modifies membrane permeability after inducible expression in *Escherichia coli* cells. J. Biol. Chem. 269, 12106–12110.

Schmidt, M., Schmidt, M.F.G., Rott, R., 1988. Chemical identification of cysteine as palmitoylation site in a transmembrane protein (Semliki forest virus E1). J. Biol. Chem. 263, 18635–18639.

Schroeder, C., Heider, H., Moncke-Buchner, E., Lin, T.I., 2004. The influenza virus ion channel and maturation cofactor M2 is a cholesterol-binding protein. Eur. Biophys. J. 34, 52–66.

Schubert, U., Ferrer-Montiel, A.V., Oblatt-Montal, M., Henklein, P., Strebel, K., Montal, M., 1996. Identification of an ion channel activity of the Vpu transmembrane domain and its involvement in the regulation of virus release from HIV-1-infected cells. FEBS Lett. 398, 12–18.

Thiel, V., Ivanov, K.A., Putics, A., Hertzig, T., Schelle, B., Bayer, S., Weißbrich, B., Snijder, E.J., Rabenau, H., Doerr, H.W., Gorbalenya, A.E., Ziebuhr, J., 2003. Mechanisms and enzymes involved in SARS coronavirus genome expression. J. Gen. Virol. 84, 2305–2315.

Torres, J., Wang, J., Parthasarathy, K., Liu, D.X., 2005. The transmembrane oligomers of coronavirus protein E. Biophys J. 88, 1283–1290.

Veit, M., Schmidt, M.F.G., 1993. Timing of palmitoylation of influenza virus hemagglutinin. FEBS Lett. 336, 243–247.

Veit, M., Schmidt, F.G., Rott, R., 1989. Different palmitoylation of paramyxovirus glycoproteins. Virology 168, 173–176.

Veit, M., Klenk, H.D., Kendal, A., Rott, R., 1991. The M2 protein of influenza A virus is acylated. J. Gen. Virol. 72, 1461–1465.

Wilson, L., McKinlay, C., Gage, P., Ewart, G., 2004. SARS coronavirus E protein forms cation-selective ion channels. Virology 330, 322–331.

Yu, X., Bi, W., Weiss, S.R., Leibowitz, J.L., 1994. Mouse hepatitis virus gene 5b protein is a new virion envelope protein. Virology 202, 1018–1023.

Yuan, X., Li, J., Shan, Y., Yang, Z., Zhao, Z., Chen, B., Yao, Z., Dong, B., Wang, S., Chen, J., Cong, Y., 2005. Subcellular localization and membrane association of SARS-CoV 3a protein. Virus Res. 109, 191–202.

Zhang, J., Pekosz, A., Lamb, R.A., 2000. Influenza virus assembly and lipid raft microdomains: a role for the cytoplasmic tails of the spike glycoproteins. J. Virol. 74, 4634–4644.